CELLO MEASUREMENTS WITH FFT IMPEDANCE ANALYSIS: DRASTIC INCREASE OF MEASUREMENT SPEED FOR ANALYSIS OF LOCAL SOLAR CELL DEFECTS

J. Carstensen, A. Schütt, and H. Föll
Institute for Materials Science, Faculty of Engineering, Christian-Albrechts-University of Kiel,
Kaiserstr. 2, 24143 Kiel, Germany, email: jc@tf.uni-kiel.de, Phone: (+49) 431 880 6181, Fax: (+49) 431 880 6178

ABSTRACT: The CELLO set up can be used to generate maps of the linear short circuit current response upon various frequencies. New implemented hard- and software allow to apply the FFT algorithm, which reduces the measurement time drastically because several maps can be obtained simultaneously from one scan. A model for the frequency dependent solar cell short circuit current impedance has been developed which allows to determine local solar cell properties like lifetime τ, back side recombination velocity S_b, and the time constant related to the $R_{ser}\,C_D$ (local serial resistance, local diode capacitance). The technique is discussed for the example of a mc-Si solar cell.
Keywords: characterization, defects, lifetime

1 INTRODUCTION

The standard CELLO (solar CELl LOcal characterization) technique analyzes the current and voltage responses of a globally illuminated solar cell to local illumination with an intensity modulated LASER beam [1 - 3]. For that measurements perturbation frequencies are used which lead to a neglectable phase shift in the response current respectively voltage. This allows for a quite simple interpretation of the measurements. In this paper quite the opposite approach will be discussed, i.e. a wide range of perturbation frequencies are chosen. To interpret the measurements the full dynamics of the solar cell has to be taken into account, but as will be shown this approach allows to extract more local parameters than any other CELLO mode. To reduce drastically the measurement time the perturbation frequencies are not applied successively but the Laser intensity is modulated by applying all frequencies simultaneously. In general this technique can be used in all CELLO modes but in this paper we will restrict the discussion to short circuit measurements without global illumination.

2 FFT-IMPEDANCE ANALYSIS

Fig. 1 shows the perturbation of four frequencies with identical amplitude P_0 which has been applied to the analog modulation input of a semiconductor Laser with a wavelength of 830 nm. An example for a possible short circuit response is shown in **Fig. 1** as well. After appropriate anti aliasing filtering this data is directly sampled by a 16 bit data acquisition board with a highest scan rate of 1 MHz. As long as the peak-to-peak amplitude P_{pp} of the Laser intensity is small enough, linear response of the solar cell can be ensured. The amplitude P_0 for each frequency in the perturbation is roughly $P_0 = P_{pp} / (2\,N)$ where N is the number of perturbation frequencies. Depending on the signal-to-noise ratio of the system, this reduction in the amplitude of each perturbation frequency limits the reasonable number of frequencies.

An FFT algorithm is used to calculate the current amplitudes $Curr(\omega_i)$ and phase shift $\phi(\omega_i)$ directly by the PC, so no lock-in amplifier is needed. The frequency dependent transfer function, called in this paper "impedance", is calculated by

$$Z(\omega_i) := \frac{Curr(\omega_i)}{P_0} \exp(i\phi(\omega_i)) = Z_0(\omega_i)\exp(i\phi(\omega_i)) \cdot \quad (1)$$

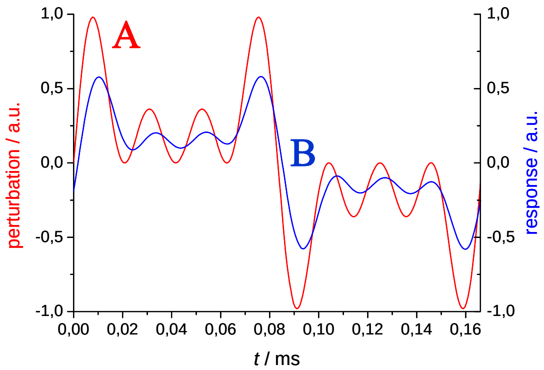

Figure 1: Curve A: Typical perturbation when applying 4 frequencies F_1 = 6 kHz, $F_2 = 3F_1$, $F_3 = 5F_1$, $F_4 = 7F_1$ with same amplitude. Curve B: possible current response.

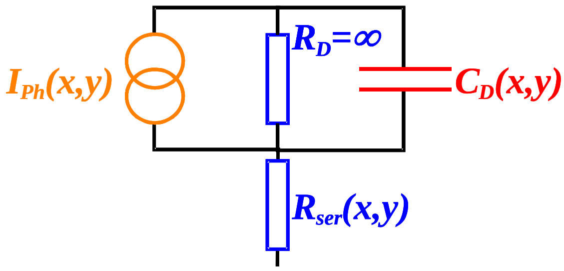

Figure 2: Model for local and global solar cell impedance at short circuit condition.

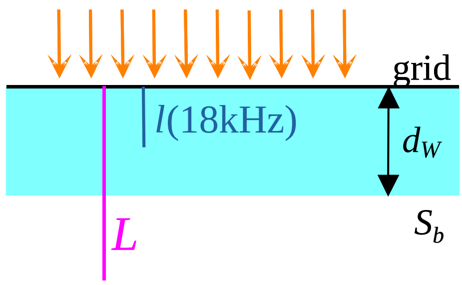

Figure 3: Typical length scales on solar cells.

3 MODELLING OF SOLAR CELL IMPEDANCE

Fig. 2 shows the most simple model for the solar cell impedance. The pn-junction diode is represented by the resistance R_D and the capacitance C_D. At short circuit conditions $R_D = \infty$ can well be assumed. Grid and back side metallization are represented by the serial resistance R_{ser}. The impedance of the electrical network of a solar cell which the photo generated current has to pass as a majority current is just

$$\frac{1}{1+i\omega R_{ser} C_D}. \quad (1)$$

The photo current is defined by generation, diffusion, and recombination in the bulk and at the back side interface. Details of the impedance related to these processes can be found e.g. in [4, 5]. Here we will only discuss, why the frequency dependent diffusion impedance analysis allows to distinguish e.g. between bulk recombination and recombination at the back side of the solar cell which is described by the surface recombination velocity S_b. The frequency dependence can be easily described by transforming the diffusion length

$$L := \sqrt{D\tau}\,, \quad (2)$$

where D is the diffusion coefficient and τ the lifetime, into an effective diffusion length $\tilde{L}$ which is defined by

$$\frac{1}{\tilde{L}} = \frac{1}{\sqrt{D}}\sqrt{\frac{1}{\tau}+i\omega}\,. \quad (3)$$

At low frequencies $\tilde{L} \to L$. For higher frequencies $\tau^{-1} \to 0$, thus a second length scale l dominates, given by

$$\frac{1}{l} := \frac{1}{\sqrt{D}}\sqrt{i\omega}\,. \quad (4)$$

Fig. 3 displays the relations for solar cells with a thickness d_W = 300 µm and a diffusion length L = 500 µm. At low perturbation frequencies the short circuit current will be sensitive to S_b because $L > d_W$. Taking a diffusion coefficient $D = 23$ cm^2 / s at 18 kHz we find an already quite small $l \approx 140$ µm, i.e. no information of the recombination at the back side of the wafer can reach the front side where the photo current is collected. So the short circuit current induced by a Laser modulation frequency of 18 kHz will not be sensitive to S_b. The Eq. (1) - (4) already allow for a qualitative understanding of the impedance data presented in this paper. The full solution of the frequency dependent diffusion equation is e.g. discussed in [5].

At short circuit conditions R_D is very large, i.e. the slope of the IV-curve is very small. This is the reason, why standard LBIC measurements are quite simple: ohmic losses dU induced by a current flow dI_{sc} through the solar cell grid and the connecting wiring do change the short circuit current significantly. But this is only true for dc currents or at low frequencies. For high frequencies the impedance of the capacitance $1/(i\omega C_D)$ becomes very small, especially if the solar cell is large. For such high frequencies an active power supply is needed to compensate for the ohmic losses.

4 EXPERIMENTAL RESULTS AND DISCUSSION

In this paper we present short circuit current impedance results for a 10 cm x 10 cm mc-Si solar cell with a thickness of 300 µm. No pure amplitude maps are shown because they look much like well known LBIC maps and they do not differ drastically as a function of applied frequency, at least not at the first glance. **Fig. 4a)** shows the ratio of two amplitude maps I_{sc}(18kHz) / I_{sc}(6 kHz). Here e.g. significant differences between the central part of the cell and an outer border some mm wide become quite obvious. If such structures become obvious for the naked eye, it will be easier to extract information by a pure mathematical approach as well. Due to this reason for the fitting of the impedance data only ratios of amplitude maps are used. As a second advantage of this approach reflectivity differences, e.g. of different grains are no problem for the interpretation of the data. Before having a closer look at the phase shift maps **Fig. 4 b) - d)** we will discuss the fitting results of **Fig. 5**. There is a very good agreement between the map of R_{ser} C_D in **Fig. 5c)** and the standard CELLO serial resistance map in **Fig. 5d)** although both maps have been extracted from completely different measurement conditions for the solar cell (which gives some confidence in the reliability of both results): Map c) from the phase shift in the short circuit current, i.e. a time delay, and map d) mainly from voltage measurements under open circuit condition. Most remarkable are the strong ohmic losses show the phase shift for the modulation frequencies of 6kHz, 18kHz, and 42kHz. In **Fig. 4d)** the dark area at the right side and the four horizontal dark lines are obvious as well. Thus there is very good agreement between the results of the standard CELLO method and this new impedance analysis technique.

The missing of the Al backside metallization around the edge of the solar cell is clearly visible in **Fig. 5b**) as well. Here S_b increases by at least one order of magnitude around the edge of the solar cell where no Al backside metallization and consequently no Al-BSF exists.

In **Fig. 5a)** the left side of the solar cell shows a significant decreased lifetime and a parallel grain boundary structure which is typical for a mc-Si wafer from the edge of a block. Interestingly in this whole area the back side surface recombination velocity S_b is large, i.e. this is a strong hint that although an Al-backside metallization exists a back surface field (BSF) did not form in this region.

The same is true for all areas in the central part of the wafer with a high dislocation density (visible in Fig. 5a) as blue areas with low life time). This anticorrelation between low lifetime and large surface recombination could be explained by charged bulk defects, which are strongly recombination active and due to their charging do not allow for the formation of a back surface field.

A last feature which should be pointed out is the bad lifetime around the edge of the solar cell. Probably it is better to state that the center of the solar cell has a very good life time due to the Al gettering.

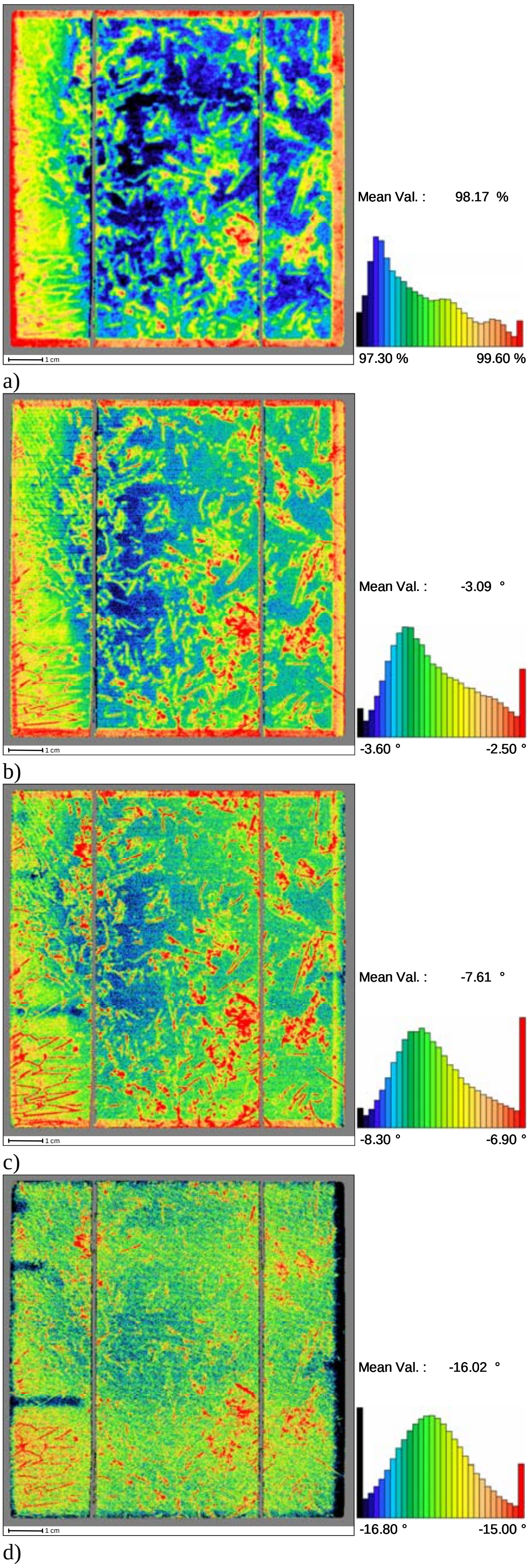

Figure 4: CELLO measurement results: a) ratio of amplitudes of short circuit currents I_{sc}(18kHz) / I_{sc}(6 kHz) at different frequencies; short circuit current phase shift maps for b) 6kHz, c) 18kHz, and d) 42kHz.

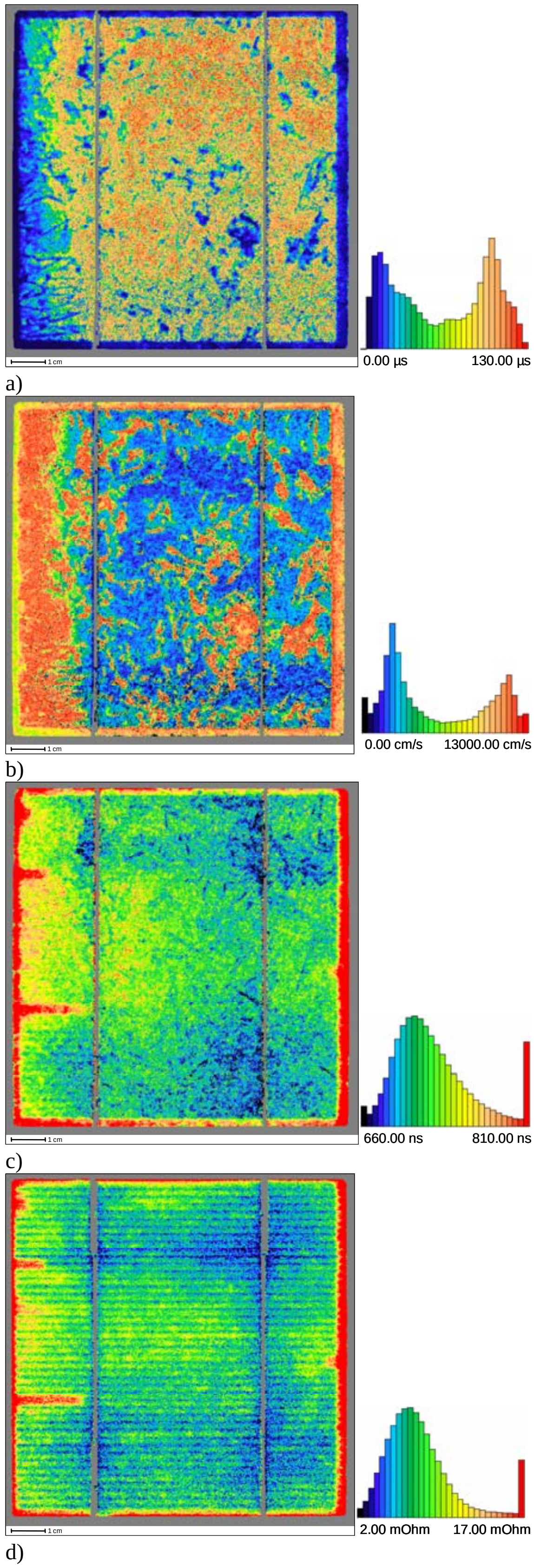

Figure 5: Resulting maps from fitting of measurements to solar cell model: a) lifetime t; b) backside surface recombination velocity S_b; c) R_{ser} C_D map. d) for comparison with c): standard CELLO R_{ser} map calculated from the open circuit voltage map.

The results in **Fig. 5a)** are a strong hint for the good efficiency of Al-gettering on this solar cell. It reduces drastically the bulk as well as the interface recombination.

Having some experience with the frequency dependent short circuit current response some of the results discussed above already could have been gained directly from the short circuit current phase shift maps of **Fig. 4b) - c)**.

As discussed in the theoretical part different defect types have different frequency dependencies which are here summarized as a rule of thumb for the frequency response of short circuit current:

I) low frequencies: τ and S_b dominate;
II) medium frequencies: τ dominates, R_{ser} C_D is visible;
III) high frequencies: R_{ser} C_D dominates, τ is visible.

Consequently, the broken grid fingers and the right border with large local serial resistance (cf. **Fig. 5c)** are clearly visible in the phase shift map at high frequency (42 kHz, **Fig. 4d**) as black areas with strong phase shift. At medium frequencies (18 kHz, **Fig. 4c**) the broken grid fingers are barely visible and they are completely invisible at low frequencies in **Fig. 4b**).

The structures related to areas of low life time in **Fig. 5a)** are clearly visible in all phase shift maps while all structures of the S_b map are only visible in the phase shift map at low frequency (**Fig. 4b**) and in **Fig. 4a)**. This last part of the discussion just clarifies how the information of different defect types is "contained" in the frequency dependent short circuit current maps and that mathematics is just needed to deconvolute this information.

5 SUMMARY AND OUTLOOK

The FFT impedance analysis of solar cells is a fast and powerful tool to characterize in detail local cell properties like τ, S_b, and R_{ser} C_D. Some of the impedance results have already been checked by independent measurements (e.g. R_{ser} map by conventional CELLO analysis) and further verification will be done in near future.

Improving the current measurement by using a potentiostat optimized for impedance analysis will lead to even better results. In the future the optimized potentiostat will be able to measure a larger variety of solar cells using the concepts and models presented here.

6 ACKNOWLEDGMENTS

This work has been supported by the German network project "Netz Diagnostik" and by DFG grant FO 258/11-1.

7 REFERENCES

[1] J. Carstensen, G. Popkirov, J. Bahr, and H. Föll, in *Proceedings of the 16th European Photovoltaic Solar Energy Conference*, VD3.35, Glasgow (2000).

[2] J. Carstensen, G. Popkirov, J. Bahr, and H. Föll, *Solar Energy Materials & Solar Cells* **76**, 599 (2003).

[3] J. Carstensen, A. Schütt, and H. Föll, in *Proceedings of the 22nd European Photovoltaic Solar Energy Conference*, 1CV.1.34, Milan (2007).

[4] A. Schütt, S. Keipert, J. Carstensen, and H. Föll, in *Proceedings of the 22nd European Photovoltaic Solar Energy Conference*, 1CV.1.35, Milan (2007).

[5] J. Carstensen, E. Foca, S. Keipert, H. Föll, M. Leisner, and A. Cojocaru, *Phys. Stat. Sol. (a)* , accepted (2008).